Journal of Mines, Metals and Fuels, *73(8): 2321-2337; 2025. DOI: 10.18311/jmmf/2025/49219*

Print ISSN : 0022-2755

Journal of Mines, Metals and Fuels

Contents available at: *www.informaticsjournals.co.in/index.php/jmmf*

Optimisation and Analysis of Laser Cutting Parameters for AISI 304 Stainless Steel: Enhancing Cut Quality and Surface Roughness

Nitin A. Kharche[1*], Vishal N. Sulakhe[1], Prasad R. Baviskar[2], Kiran Kaware[1] and Kamalkishor G. Maniyar[3]

[1]Department of Mechanical Engineering, School of Engineering and Technology, Sandip University, Nashik - 422213, Maharashtra, India; latestresearch22@gmail.com

[2]Department of Mechanical Engineering, Late Sau. Kantabai Bhavarlalji Jain College of Engineering, Chandwad, Nashik - 423101, Maharashtra, India

[3]Department of Mechanical Engineering, Dr. D. Y. Patil Institute of Technology, Pimpri, Pune - 411018, Maharashtra, India

Abstract

This study seeks to determine the ideal parameters for laser cutting to improve kerf measurements and surface finish in AISI 304 stainless steel. The CO2 laser cutting machine (AMADA FO-3015NT) had its key process parameters, such as laser power, cutting speed, assist gas pressure, and focal position. The effects of these parameters were examined on kerf width, kerf taper, and surface roughness for different material thicknesses of 1.5mm, 2mm, and 2.5mm, respectively. The analysis was performed to establish an ideal cutting method by employing Response Surface Methodology (RSM) and Analysis of Variance (ANOVA). The kerf width, taper, and surface roughness were significantly influenced by laser power and cutting speed, as indicated by the results obtained. Increased laser power augmented the kerf width and surface roughness, while elevated cutting speed diminished both kerf width and roughness. The optimal kerf efficiency and superior taper geometry were achieved with a laser power of 3 kW, a cutting speed of 4500 mm/min, and a gas pressure of 0.8 MPa.

Major findings: *The Kerf width and taper were often reduced for curved profiles as compared to straight profiles, while surface finish quality improved with higher cutting speed and optimal gas pressure. This study envisages a comprehensive investigation of the influence of laser cutting parameters on the cuts produced in AISI 304 stainless steel that assists producers in optimising cut quality for industrial applications.*

Keywords: *ANOVA, AISI 304, CO2 Laser, Kerf Width, Laser Cutting, Process Parameters, Stainless Steel, Surface Roughness*

1.0 Introduction

Laser cutting is a well-known technique in the fabrication and production industries as it provides high productivity and accuracy in the processing of a variety of materials. AISI 304 is a prominent material used in a wide range of sectors and goods, including medical and automotive applications[1,2]. The state of the cut section and the resulting surface polish are the crucial parameters influencing the behaviour and durability of these parts. Adjusting the laser cutting settings to an appropriate value is crucial for achieving an excellent cut edge and surface finish[3,4]. The published literature focused on how various laser cutting parameters, like cutting speed and feed rate, affect the residual stresses and surface smoothness of a variety of steel alloys[5,6]. However, the impact of these

**Author for correspondence*

characteristics on AISI 304 stainless steel has not been explored. It is found that an additional study needs to be explored to understand the relationship between cutting parameter settings and surface roughness to gain a better understanding of laser cutting for this material[7,8]. Several studies published in the literature have looked into the influence of cutting parameters on the residual stresses in machined steel parts[9,10]. This study found that adjusting the cutting speed or feed rate impacts the residual stresses in the completed machined surface[11,12]. Furthermore, the properties of the tool material and coatings influence the distribution of residual stresses. Previous studies on laser cutting of enhanced high-strength steel have looked at the impact of sheet thickness and material coating on cutting parameters and material damage severity[13,14]. The variability of cutting parameters was found to be less influential than sheet thickness and material coating. Another study on AISI 316L steel discovered that residual stresses caused by orthogonal cutting are determined by the geometrical properties of the cutting tool and the machining conditions[15,16].

A thorough literature analysis was conducted to determine how various laser-cutting elements influence the process outcome. To be more specific, Jadhav and Kumar investigated the influence of laser power, cutting speed, and assist gas pressure, and discovered that increasing laser power and gas pressure reduced surface roughness while increasing cutting speed caused edge defects[17,18]. Even with complicated surface topography, fatigue strength loss caused by surface imperfections remains an issue. According to Pessoa *et al*., cutting AISI 304 stainless steel parts using a laser reduces fatigue strength by 40% because to the notch effect of burrs and pores created during the laser cutting process[19,20]. This is especially detrimental to components subjected to cyclic loads, as stress concentrations at these flaws frequently result in early failure[21,22].

Numerous research has investigated the effect of laser cutting parameters on the surface condition and microstructure of AISI 304 stainless steel. It has been recommended that thermal input be regulated during laser cutting to produce improved surface quality and microstructural qualities of the material[23,24].

1.1 Aim and Objectives of the Research

The goal was to reduce kerf width, taper, and surface roughness, resulting in clean and precise edges. An extensive study has also been undertaken to determine the thermal and mechanical impacts of laser cutting.

Several studies have examined the thermal effects of laser cutting on metals and investigated the mechanical consequences on high-strength alloys, such as AISI 304 stainless steel[25,26]. Further research has analysed the behaviour of various stainless-steel varieties and their laser cutting performance, revealing the particular performance profile of AISI 304. Similarly, Authors investigated the effects of laser cutting on the surface finish of stainless steel, emphasising the importance of including post-processing treatments to increase the quality of the cut surface[27,28]. More complex techniques, such as multi-objective optimisation through genetic algorithms, as employed, have proven that it is possible to improve the laser cutting of stainless steel and achieve a better cut edge. Other experimental studies have stressed the vital relevance of careful process parameter control in minimising surface roughness during laser cutting of stainless steel[29,30]. Finally, to improve laser cutting of thin steel sheets, Tsai used the Taguchi technique, which provides a statistical foundation for improved cut quality. Their findings demonstrated that in all cutting applications, it is critical to optimise all cutting parameters to achieve the optimum outcomes in terms of both performance and surface quality[31,32].

1.2 Literature Summary

This study was carried out to optimise laser cutting parameters for AISI 304 stainless steel to improve kerf size and surface quality. Precision cuts with minimal material deformation and high-quality surface finishes are critical in industrial settings. Key parameters such as laser power, cutting speed, assist gas pressure, and focal location were systematically adjusted to see how they affected kerf breadth, kerf taper, and surface roughness[33,34]. The experiment employed RSM and ANOVA to model the correlations between laser cutting parameters, kerf dimensions, and surface quality[35,36]. This statistical research revealed the best cutting settings for precise and high-quality cuts in various thicknesses of AISI 304 stainless steel. The findings offer useful insights into optimal laser cutting conditions, assisting industry practitioners in selecting the most effective parameters for the required cut quality[37,38].

2.0 Materials and Methods

2.1 Materials

The material employed in this investigation was AISI 304 stainless steel, which is widely selected due to its outstanding corrosion resistance, high strength, and formability. It is ideally suited to the automotive, aerospace, and construction industries, where strength and accuracy are essential success elements[39,40]. This experiment used AISI 304 stainless steel sheets of three different thicknesses: 1.5mm, 2mm, and 2.5mm. These thicknesses were chosen to investigate the impact of material thickness on kerf width, taper, and surface roughness during laser cutting. Chemical composition of AISI 304 stainless steel: The chemical composition of the AISI 304 stainless steel used in this study is shown in Table 1.

The presence of chromium and nickel offers AISI 304 the correct measure of corrosion resistance it possesses, whereas the low carbon presence makes the AISI 304 easier to weld with minimal carbide formation during the welding of the steel. In this study, these chemical properties helped to track how the behaviour of the material under the laser cutting process especially the laser power, cutting speed, and gas pressure[41,42].

2.2 Experimental Setup

Laser Cutting Machine: AMADA FO-3015NT: The laser cutting experiments were performed with the help of a CO2 laser cutting machine by using AMADA and model FO-3015NT. This machine is specialised in cutting various materials in the market with high speed and accuracy, especially steel such as stainless steel[43,44]. It uses a CO2 laser source, which works by using an electric discharge to make CO2 gas emit a laser beam intensely. The specifications of the AMADA FO-3015NT used in the experiment are as follows: Laser Type: CO2 Laser, Maximum Laser Power: 4000W (power adjustable), Wavelength: 10.6µm, Work Area: 3000mmx1500mm, Cutting Thickness Capability: up to 20mm mild steel and 10mm stainless steel, Maximum Cutting Speed: variable up to 20m/min depending on material and thickness[45,46]. Focus Control: The system automatically positions the focal point to ensure the laser cutting head adopted for the experiment is presented in Figure 1.



Figure 1. Shows the AMADA CO2 laser cutting head.

Table 2. Test conditions for laser cutting of AISI 304 stainless steel

Parameter	Values Tested
Laser Power (W)	2000W, 3000W, 4000W
Cutting Speed (mm/min)	3500 mm/min, 4500 mm/min, 5500 mm/min
Assist Gas	Nitrogen
Assist Gas Pressure (MPa)	0.7 MPa, 0.8 MPa, 0.9 MPa
Focal Position (mm)	-1.5mm (below surface)
Material Thickness (mm)	1.5mm, 2.0mm, 2.5mm
CO2 Laser Machine	AMADA FO-3015NT
Wavelength	10.6µm
Work Area	3000mm x 1500mm

The following input parameters were varied to study their impact on the cut quality of AISI 304 stainless steel sheets (Table 2).

Table 2 consolidates the various parameters adjusted during the experiments to study their effects on kerf width, kerf taper, and surface roughness[47,48].

Table 1. The material primarily consists of the following elements

Component	C	Mn	Si	S	P	Cr	Ni
Wt.%	0.053	1.39	0.50	0.013	0.018	18.37	8.44

Table 3. Summary of measurement tools and techniques

Parameter	Tools	Particulars
Top/Bottom Kerf Width	Tool Maker's Microscope	Visual inspection and measurement at three locations along the cut, the average is taken for the final value
Surface Roughness (Ra)	Mitutoyo Surf Test SJ-410	Stylus-based surface tracing, measurements at three locations along the cut, and average Ra value calculated
Kerf Taper	Calculation from kerf width	$\text{Kerf aper}(\circ) = \left(\frac{Top\ Kerf\ \ of\ \ Width - Bottom\ Kerf\ \ Width}{Materials\ \ Thickness} \right)$

2.3 Measurement

In this study, measurements of kerf width (top and bottom), kerf taper, and surface roughness were critical in determining the impact of laser cutting parameters on the quality of AISI 304 stainless-steel cuts. Table 3 specifies the measurement methodologies and tools employed, which are explained below. Table 3 gives a quick review of instruments and approaches[49,50].

3.0 Experimental Design

3.1 Process Parameters

Several critical input parameters were employed to regulate the laser cutting process, including laser power, cutting speed, assist gas pressure, and the focal length of the cutting lens[51,52]. These factors were systematically changed to determine how they affected the kerf width, kerf taper, and surface roughness in AISI 304 austenite stainless steel[53,54]. The top and lower limits of each parameter were determined using empirical investigations and the physical limitations of the CO2 laser cutting equipment (AMADA FO-3015NT). The accompanying Table 4 shows the above- mentioned process parameters with the variation ranges used in the experiment[55,56]. Figure 2 depicts a macro view of straight and curved profiles.

3.2 Statistical Analysis

In this study, laser cutting parameters such as laser power, cutting speed, and frequency of oscillation were used as process variables to determine their effects on output responses such as kerf width, kerf taper, and surface roughness using RSM and ANOVA[57,58].

3.2.1 Response Surface Methodology (RSM)

RSM is a statistical method used in optimisation strategies that considers numerous input elements. They make it easier to determine the relationships between process parameters and responses while also providing the ideal circumstances for the observed outcomes[59,60]. The responses comprised Top Kerf Width, Bottom Kerf Width, Kerf Taper, and Surface Roughness, and their specifications are shown in Table 5.

Table 4. Process parameters considered for the experiment

Process Parameter	Range Tested
Laser Power (W)	2000 W, 3000 W, 4000 W
Cutting Speed (mm/min)	3500 mm/min, 4500 mm/min, 5500 mm/min
Assist Gas Pressure (MPa)	0.7 MPa, 0.8 MPa, 0.9 MPa
Focal Position (mm)	-1.5 mm (below surface)

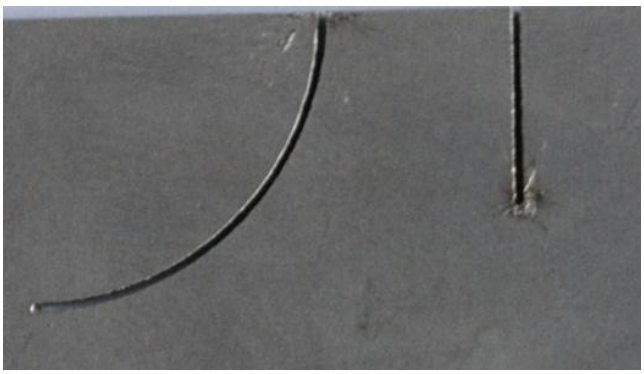


Figure 2. Macro image of straight and curved profile.

3.2.2 ANOVA (Analysis of Variance)

The ANOVA technique was used to analyse the statistical significance of process parameters and their interactions for all process responses, revealing which parameters had the greatest influence on the response[61,62]. The primary interactions between laser power, cutting speed, and assist gas pressure on response characteristics were

Table 5. Specification of surface roughness tester

Equipment Name	Surf Test
Make	SJ-210- MITUTOYO
Measuring range	17.5mm
Measuring speed	0.25-0.75 mm/sec
Cut to length	0.08, 0.25, 0.8, 2.5mm
Sampling length	0.08, 0.25, 0.8, 2.5mm
Stylus tip radius	2µm
Type of indenter	Diamond
Power supply	Battery and AC adapter
Mass	500g

identified. According to the results, these parameters were determined to be significant, with a low p-value indicating a factor effect[63,64]. Quadratic regression models for predicting minimal kerf width, taper, and surface roughness were created and experimentally validated using RSM and ANOVA data[65,66].

4.0 Results and Discussion

4.1 Kerf Width and Taper

Kerf width (top and bottom) and kerf taper are important features of laser cutting because they determine cutting accuracy and surface quality. During trials on AISI 304 stainless steel sheets of varying thicknesses (1.5mm, 2mm, and 2.5mm), laser power, cutting speed, and gas pressure were identified as the key parameters influencing kerf dimensions[67,68].

4.1.1 Effect of Laser Power

Laser power is one of the parameters that determines the width of the kerf. Higher laser power often results in the delivery of more energy to the material and thus the size of the molten zone[69,70]. This leads to an increase in the sizes of kerf width at the top and below the line of symmetry. An increase in top and bottom kerf widths for all the thicknesses of AISI 304 sheets is observed with an increase in laser power from 2000W to 4000W.

- At 2000W, the top kerf width using a 1.5mm AISI 304 sheet has a mean of 0.478mm while the bottom kerf width has a mean of 0.438mm.
- At 4000W top kerf width is found to be 0.486mm, and the bottom kerf width is found to be 0.416mm as the material melts and gets expelled at a higher rate at higher energy levels.

The same is true of thicker sheets, that is, the amount of energy corresponding to the sheet thickness increases in the same proportion to the basic value. It not only widens the kerf at the top but also enhances the tapering effect, in which the variation of the upper and lower kerf width expands as the thickness increases[71,72].

4.1.2 Tables of Experimental Results

Below are Tables 6 and 7, which are representative experimental results for kerf width and taper for AISI 304 under different conditions:

The experimental table analysis shows that, of all the measured parameters, laser power and cutting speed have the largest influence on the final kerf width and taper. The 2D profiles show that increased laser power causes increased kerf width and taper, resulting in less precise cuts. On the other hand, raising the cutting speed reduces kerf width and taper, but it has a negative impact on the surface finish. The assist gas pressure is also important in reducing kerf width since it effectively removes molten material, while increasing pressure has a significant impact on surface finish. According to the findings, the following parameters are best for AISI 304 stainless steel to produce the least kerf width and taper while maintaining good surface roughness: laser power of 3000W, cutting speed of 4500 mm/min, and gas pressure of 0.8 MPa. Aside from studying the effects of laser power, cutting speed, and gas pressure on kerf width and taper in straight profile cuts, the same experiments were carried out for curved profile cuts. The results show that the thickness of AISI 304 stainless steel has a substantial impact on kerf width and taper behaviour for straight and curved geometries[73].

4.1.3 Effect of Cutting Speed

Cutting speed is a parameter that greatly influences the amount of time that the laser beam spends in contact with the material. The author argues that when the cutting speed is lower, it signifies that more energy is being transferred to the material, which implies that the kerf width will be wider. On the other hand, at higher cutting speeds, the time for two interfaces to meet is smaller and thus, the width of kerfs is also small.

Table 6. Experimental plan and results for AISI 304 (1.5mm Straight Profile)

Sno.	Power (W)	Cutting Speed (mm/min)	Gas Pressure (MPa)	Top Kerf Width (mm)	Bottom Kerf Width (mm)	Kerf Taper (°)	Surface Roughness (µm)
1	3000	5500	0.7	0.4571	0.4271	0.5732	1.621
2	**3000**	**3500**	**0.9**	**0.4682**	**0.4289**	**0.751**	**1.692**
3	3000	4500	0.8	0.4739	0.4294	0.8503	1.659
4	4000	4500	0.9	0.4841	0.4139	1.3414	2.431
5	2000	4500	0.7	0.4784	0.4385	0.7624	2.589
6	3000	4500	0.8	0.4699	0.4302	0.7586	1.789
7	3000	4500	0.8	0.4679	0.4284	0.7548	1.714
8	4000	3500	0.8	0.4883	0.4187	1.3299	2.509
9	2000	5500	0.8	0.4733	0.4327	0.7758	2.019
10	2000	4500	0.9	0.4761	0.4359	0.7682	2.012
11	3000	5500	0.9	0.4554	0.4250	0.5809	1.651
12	3000	4500	0.8	0.4676	0.4304	0.7108	1.733
13	3000	3500	0.7	0.4714	0.4305	0.7815	1.765
14	4000	5500	0.8	0.4871	0.4173	1.3338	2.209
15	2000	3500	0.8	0.4798	0.4394	0.772	2.019
16	3000	4500	0.8	0.4701	0.4298	0.7701	1.822
17	4000	4500	0.7	0.4861	0.4161	1.3376	2.309

Table 7. Experimental plan and results for AISI 304 (2mm curved profile)

Sno.	Power (W)	Cutting Speed (mm/min)	Gas Pressure (MPa)	Top Kerf Width (mm)	Bottom Kerf Width (mm)	Kerf Taper (°)	Surface Roughness (µm)
1	3000	5500	0.7	0.4451	0.3861	0.8455	1.727
2	3000	3500	0.9	0.4562	0.3877	0.9817	1.824
3	3000	4500	0.8	0.4617	0.3884	1.0505	1.782
4	4000	4500	0.9	0.4721	0.3729	1.4217	2.563
5	2000	4500	0.7	0.4664	0.3975	0.9874	2.721
6	3000	4500	0.8	0.4579	0.3892	0.9846	1.921
7	3000	4500	0.8	0.4559	0.3874	0.9817	1.846
8	4000	3500	0.8	0.4763	0.3779	1.4102	2.632
9	2000	5500	0.8	0.4613	0.3917	0.9975	2.145
10	2000	4500	0.9	0.4641	0.3949	0.9917	2.134
11	3000	5500	0.9	0.4431	0.3840	0.847	1.783
12	3000	4500	0.8	0.4556	0.3894	0.9487	1.865
13	3000	3500	0.7	0.4592	0.3895	0.9989	1.897
14	4000	5500	0.8	0.4751	0.3763	1.4159	2.341
15	2000	3500	0.8	0.4678	0.3984	0.9946	2.142
16	3000	4500	0.8	0.4581	0.3888	0.9932	1.954
17	4000	4500	0.7	0.4741	0.3752	1.4174	2.432

- At a cutting speed of 3500 mm/min, the top kerf width is 0.471 mm, and the bottom kerf width is 0.430mm for a 1.5mm sheet of AISI 304.
- Increasing the speed to 5500 mm/min results in a smaller top kerf width of 0.45mm, with the bottom kerf width reduced to 0.427mm.

This pattern is observed across all thicknesses, with the cutting speed inversely affecting the kerf width. For thicker materials (2mm and 2.5mm), the effect of cutting speed is more pronounced, and a high cutting speed reduces kerf widths significantly. This is due to the reduced time for material melting, which minimises kerf formation.

4.1.4 Effect of Gas Pressure

Auxiliary gas pressure (in this case, nitrogen) aids in the ejection of molten material from the kerf and has a considerable impact on cooling the cutting edge. The experimental data show that increasing the assist gas pressure reduces the kerf breadth because it aids in the correct evacuation of the molten material.

- At 0.7 MPa, the width of the kerf at the top is 0.467mm, whereas the width of the kerf at the bottom is 0.430mm for a 1.5mm-thick AISI 304 sheet.
- As the gas pressure increases to 0.9 MPa, the top kerf width is cut down to 0.455mm whilst the bottom kerf width is cut down to 0.425mm.

However, high gas pressure causes turbulence in the molten pool and leads to a rough-cut surface with an uneven kerf taper. Thus, moderate gas pressure appears to be most effective for achieving the desired kerf width and taper at the same time.

4.1.5 Kerf Taper

Kerf taper is understood as the variation in kerf thickness from top to bottom. Larger kerf taper means the difference in the top and bottom widths are larger and they are likely caused by incorrect parameter settings. It is clear from the results that both laser power and cutting speed influence the kerf taper.

- At a laser power of 2000W and cutting speed of 3500 mm/min, the kerf taper of a 1.5mm sheet is moderate at 0.7815°.
- The kerf taper increases to 1.3414° with high laser power (4000W) and the same cutting speed, which means that the higher power increases the material melting at the top, and as a result, the kerf at the top is larger than the bottom.

At higher scribing speeds, the kerf taper is reduced because the cutting edges have contact with the work piece for a very short time hence, kerf on the top is almost equal to that on the bottom. The best cutting speed and laser power for minimum kerf taper were determined to be at 3000W and 4500 mm/min.

4.1.6 Effect of Profile Type on Kerf Width

When comparing the kerf widths of straight and curved profiles, it was discovered that in the case of curved profiles, all thicknesses revealed slightly reduced kerf widths at both the top and bottom. This is due to the fact that the laser beam goes continuously around the curved profile, resulting in continuous material removal.

- In case of a straight profile, the top kerf width for a 1.5mm thick AISI 304 sheet was 0.4679mm and for a curved profile it was 0.4454mm.
- The same trend was observed when a 2mm thick sheet was used with a top kerf width of 0.4556mm for the straight profile and 0.4332mm for the curved profile.

The more consistent decrease of kerf width for curved profiles indicates that laser intensity in curved cuts is more auspicious and unswerving because of the continuous velocity of the laser beam along the curved cut path, thus avoiding localised heat, which leads to material swelling.

4.1.7 Effect of Profile Type on Kerf Taper

As in the case of the kerf taper, which is the difference in the top and bottom kerf width. Overall, the studies revealed that the kerf taper was relatively smaller in curved profiles as compared to straight profiles. I believe that the slower motion of the laser along the curve is beneficial in that it produces less taper by evenly melting the material.

- The kerf taper for the straight profile for a 1.5 mm thick sheet was found to be 0.7548°, while for the curved profile, the kerf taper was found to be 0.7357°.

- For the thickness of 2mm, the kerf taper for the straight profile was found to be 0.9817 degrees, and for the curved profile was 0.9358 degrees.

The results indicated that the reduction in kerf taper for curved profiles is much greater than thinner sheets, in particular for thicker ones. This suggests that curved profile cutting, though challenging, can produce enhanced kerf profile accuracies with closer top and bottom widths than angular deviations.

4.1.8 Impact of Material Thickness on Straight and Curved Profiles

The results also reveal that straight and curved profiles for increasing thickness of AISI 304 sheet have larger kerf width and kerf taper. However, it is seen that the relative difference between straight and curved profiles is approximately constant for these thicknesses. As the thickness of the material increases, it becomes increasingly difficult to control the laser beam to cut through the material, resulting in wider kerf and greater taper, however, curved profiles are made with smaller taper than the straight profiles.

- For the 2.5 mm-thick sheets, the top kerf width obtained for a straight profile was measured to be 0.4379mm with a taper of 1.0169°.
- For the curved profile, the Kerf width at the top profile was 0.4157mm, and the taper was 1.0250°.

These findings indicate that for thicker materials, curved profiles yield a benefit with decreasing kerf widths and taper angles, thus achieving greater accuracy and product quality.

4.1.9 Surface Roughness

Figure 3 depicts the effect of laser cutting process settings on the top kerf width of AISI 304 stainless steel with a 2mm thick straight profile. The picture is made up of three subplots, each demonstrating the link between two process parameters. Figure 3 (a) depicts the top kerf width interaction between cutting speed and laser power, with greater laser power levels somewhat expanding the kerf width, particularly at lower cutting rates. On the other hand, the top kerf width decreases as cutting speed increases, implying that greater speeds limit heat input,

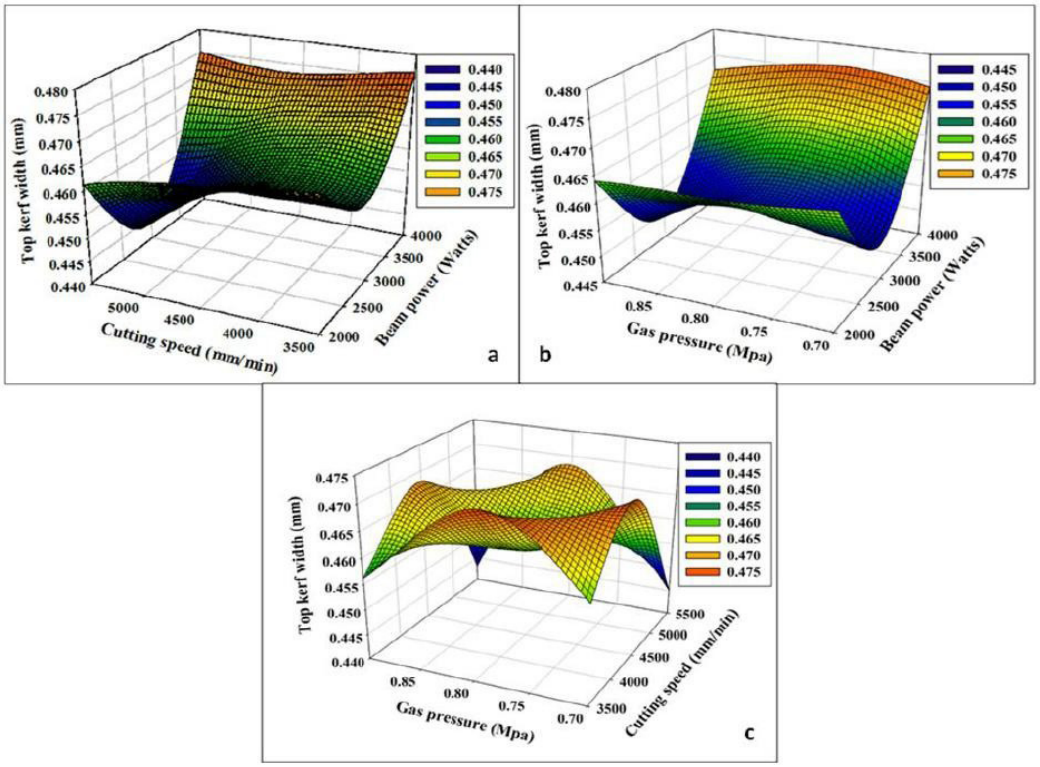


Figure 3. Effect of process parameter on top kerf width for AISI 304: 2 mm thickness straight profile.

resulting in narrower kerf widths. As shown in Figure 3 (b), the combined effect of assist gas pressure and laser power reduces the growth in top kerf width with assist gas pressure, but only when the laser power is kept low. Figure 3 (c) depicts the interaction of cutting speed and assist gas pressure on top kerf width, demonstrating that the top kerf width decreases as cutting speed and assist gas pressure increase. The results are consistent with past discourse, pointing to the fact that to attain the least kerf width for greater accuracy, cutting speed and assist gas pressure must be increased**.**

Figure 4 depicts the effect of laser cutting process settings on kerf taper in AISI 304 stainless steel with a 2mm thick straight profile. The kerf taper measures how much the width of the cut changes from top to bottom, with greater values indicating a more curved cut rather than a straight, vertical cut. Figure 4 is broken into three parts (a, b, and c), each representing the interaction of two process factors. Figure 4 (a) shows a link between cutting speed and laser power on kerf taper. As laser power increases, so does the amplitude of the taper in all scenarios with low cutting velocities. That is, at greater speeds, the taper is lower, indicating that higher speeds do not allow for significant variance between the top and bottom kerf, resulting in better cuts. As shown in Figure 4(b), the assist gas pressure affects laser power. It was discovered that increasing laser power causes the kerf taper to increase rapidly, and that raising gas pressure reduces the effect of the increased kerf taper. Figure 4 (c) shows that kerf taper is inversely related to cutting speed and gas pressure, confirming that increased cutting speed combined with higher-pressure gas produces a straighter cut. However, it has been noted that a combination of cutting speed and gas pressure can provide slightly higher taper values.

Figure 5 shows reaction surface graphs demonstrating the impact of laser cutting settings on top kerf width for 2mm thick curved AISI 304 stainless steel. The graph above comprises three subplots (a, b, and c) that depict the interrelationship of various process factors and their impact on top kerf width. Figure 5 (a) displays the relationship between cutting speed and laser power, and the overall kerf width narrows as cutting speed increases. When the cutting speed is modest, increasing laser power results in a wider kerf breadth because more energy is applied to the material, causing more material

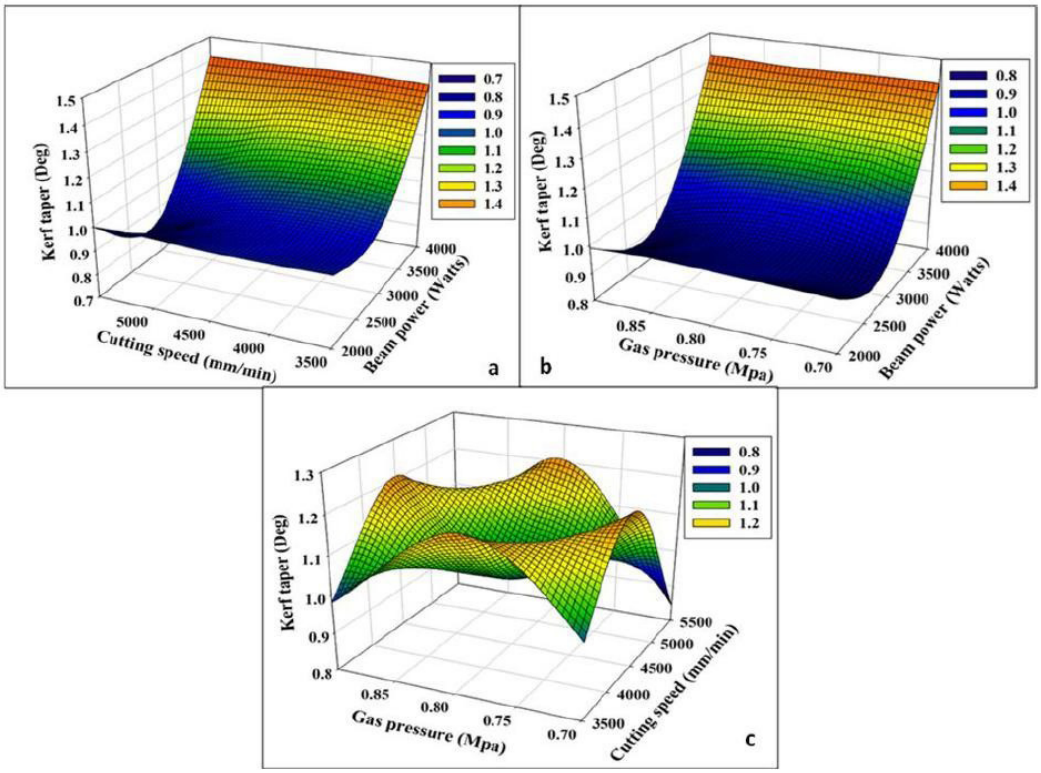


Figure 4. Effect of process parameter on kerf taper for AISI 304: 2mm thickness straight profile.

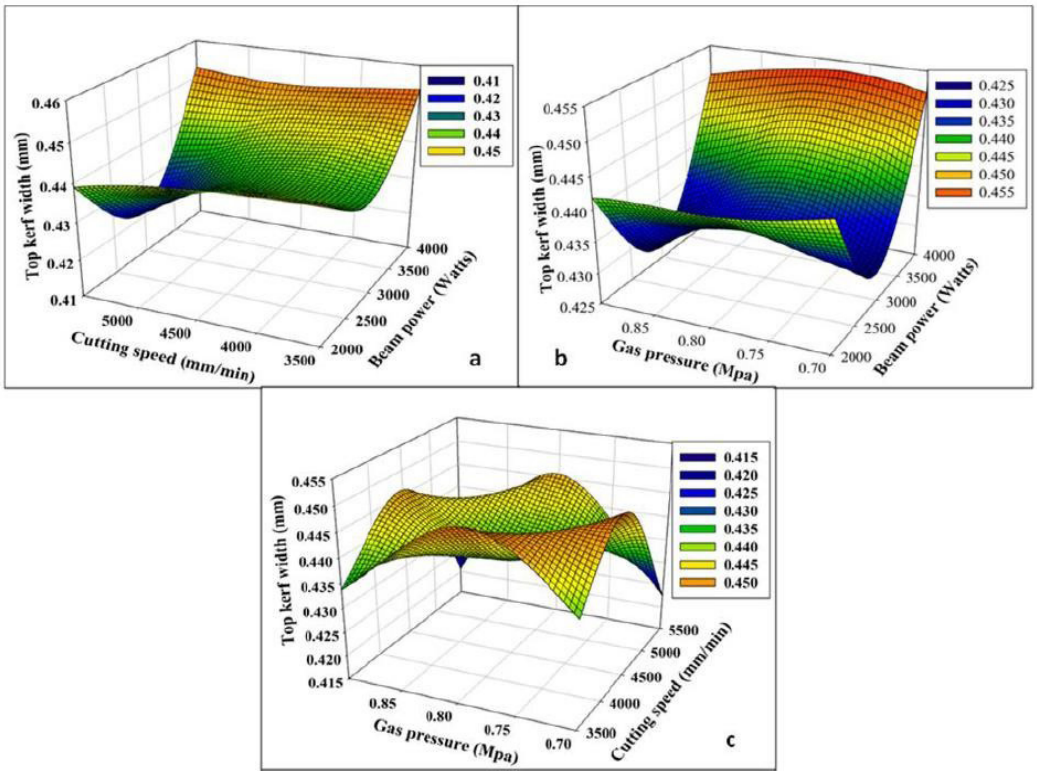


Figure 5. Top kerf width response surface graph for AISI 304: 2mm thickness curved profile.

to melt. Figure 5 (b) displays the trend of gas pressure and laser power, demonstrating that a minor increase in gas pressure causes a decrease in top kerf width, particularly at lower laser power levels. However, as the laser power increased, so did the kerf breadth due to an increase in heat supply to the material. Figure 5 (c) depicts the interaction of gas pressure and cutting speed on top kerf width, with the results indicating that as the speed of cutting increases, the kerf width narrows, and that increased gas pressure has a favourable effect on this happening. As a result, Figure 5 shows that the top kerf width of curved AISI 304 stainless steel profiles is mostly determined by laser power, cutting speed, and gas pressure.

Figure 6 depicts the effect of process parameters on kerf taper in AISI 304 stainless steel with a 2mm thick curved profile. Three subplots influence the kerf taper, which is a measure of how far a straight vertical cut diverges. The first subplot shows the relationship between cutting speed and laser power, with rising laser power resulting in higher kerf taper, especially when cutting speeds are low. However, when the cutting speed increases, the taper decreases, implying that high cutting speeds reduce taper by limiting heat input while improving cut accuracy. The second subfigure depicts the effect of assist gas pressure and laser power on kerf taper, demonstrating that gas pressure helps to reduce kerf taper, especially when laser power is low. However, when the laser power increases, so does the taper owing to increased heat input, and the top and bottom kerf widths are bigger than the centre width. The third subplot is relative to both and demonstrates how high cutting speed and gas pressure aid in reducing kerf taper or maintaining more vertical cuts. This insight is useful in situations when high-quality cutting requires maintaining the kerf taper's low coefficient of variation.

4.2 ANOVA Results

The ANOVA (Analysis of Variance) method is used to assess the impact of process parameters (laser power, cutting speed, assist gas pressure, and focus position) on the three primary response variables: The experimental examination comprises kerf width, kerf taper, and surface roughness. The statistical analysis of the findings is useful in discovering which elements have a major impact on

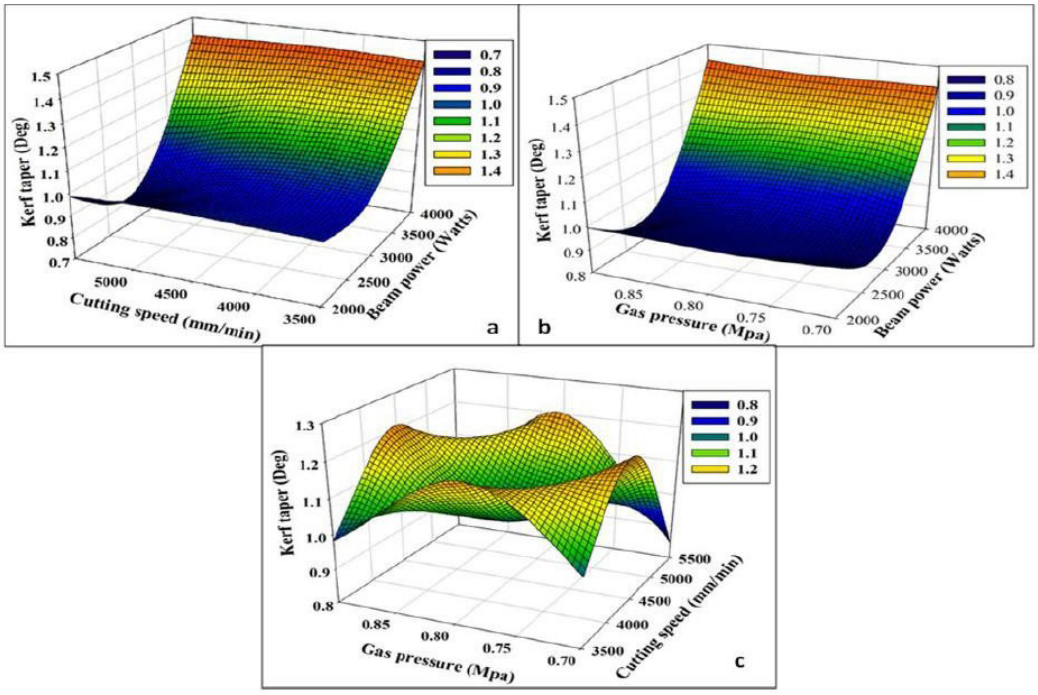


Figure 6. Effect of process parameter on kerf taper for AISI 304: 2 mm thickness curved profile.

each response, and hence which parameters should be tuned to produce the optimum cutting quality.

4.2.1 ANOVA for Kerf Width

4.2.1.1 Top Kerf Width

ANOVA of top kerf width shows that laser power (A), cutting speed (B), quadratic laser power (A^2), and gas pressure (C^2) are significant factors affecting top kerf width.

The model has a high R^2=0.9480 to suggest that these factors can accurately predict the kerf width. Laser power and cutting speed are the two most influential parameters, while the effect of the gas pressure is less crucial for the top kerf width.

4.2.1.2 Bottom Kerf Width

The ANOVA of the bottom kerf width indicated that laser power, cutting speed, and gas pressure are important factors. The quadratic effect of laser power (A^2) is also a contributing factor towards the bottom kerf width.

The bottom kerf width model achieved an R2 of 0.9870, indicating that it is highly predictive. As expected, laser power is the most influential factor, followed by cutting speed and argon gas pressure. The results show that the bottom kerf width increases approximately quadratically with laser power, implying that laser power has a nonlinear effect on the bottom kerf width.

Table 8. ANOVA for the top Kerf width of AISI 304 (2 mm thickness, straight profile)

Source	Sum of Squares	Df	Mean Square	F Value	p-value (Prob > F)
Model	0.0014	9	0.0001	14.1728	0.0010
A (Power)	0.0001	1	0.0001	16.4541	0.0048
B (Cutting Speed)	0.0001	1	0.0001	13.8790	0.0074
C (Gas Pressure)	1.1E-05	1	1.1E-05	0.9855	0.3539
A^2 (Quadratic)	0.0009	1	0.0009	89.6147	< 0.0001
C^2 (Quadratic)	6.6E-05	1	6.6E-05	5.9734	0.0445
Residual	7.7E-05	7	1.1E-05		

Table 9. ANOVA for the bottom Kerf width of AISI 304 (2mm thickness, straight profile)

Source	Sum of Squares	Df	Mean Square	F Value	p-value (Prob > F)
Model	0.0008	9	9.8E-05	58.8248	< 0.0001
A (Power)	0.0008	1	0.0008	483.6330	< 0.0001
B (Cutting Speed)	3E-05	1	3E-05	17.8323	0.0039
C (Gas Pressure)	9.7E-06	1	9.7E-06	5.8228	0.0466
A^2 (Quadratic)	1.9E-05	1	1.9E-05	11.5179	0.0115
Residual	1.2E-05	7	1.7E-06		

Table 10. ANOVA for Kerf Taper of AISI 304 (2mm thickness, straight profile)

Source	Sum of Squares	Df	Mean Square	F Value	p-value (Prob > F)
Model	0.6357	9	0.0706	29.7624	< 0.0001
A (Power)	0.3586	1	0.3586	151.1340	< 0.0001
B (Cutting Speed)	0.0097	1	0.0097	4.1133	0.0821
A^2 (Quadratic)	0.26219	1	0.26219	110.478	< 0.0001
Residual	0.0166	7	0.0023		

Table 11. ANOVA for surface roughness of AISI 304 (2mm thickness, straight profile)

Source	Sum of Squares	Df	Mean Square	F Value	p-value (Prob > F)
Model	1.6074	9	0.1786	15.6217	0.0008
A (Power)	0.0852	1	0.0852	7.4593	0.0293
B (Cutting Speed)	0.0311	1	0.0311	2.7223	0.1429
C (Gas Pressure)	0.0279	1	0.0279	2.4460	0.1618
A^2 (Quadratic)	0.1289	1	0.1289	11.2724	0.0121
B^2 (Quadratic)	0.0056	1	0.0056	2.3926	0.1658
Residual	1.2E-05	7	1.7E-06		

4.2.2 ANOVA for Kerf Taper

The analysis of the variance of kerf taper shows that the laser power (A) and its second-order term (A2) are extremely important and have the greatest influence on the taper. Furthermore, it was discovered that cutting speed (B) has a moderate effect, whereas gas pressure has a minor effect on the process.

The R2 value of 0.9418 indicates that the model can reliably predict kerf taper. Power is the most important component influencing the taper, and the quadratic effect of power reinforces this relationship.

4.2.3 ANOVA for Surface Roughness

Surface roughness is a critical metric that defines the quality of the cut surface. The analysis of variance (ANOVA) indicates that laser power (A), cutting speed (B), and gas pressure (C) are the determinants of surface roughness. Additional second-order interactions, specifically, the square of laser power (A2) and the square of cutting speed (B2), are also noteworthy.

The coefficient of determination $R^2 = 0.9480$ indicates that the constructed model is effective in predicting surface roughness. The findings indicate that laser power predominantly affects surface roughness, whereas cutting speed and gas pressure also exert considerable influence. The interaction terms (e.g., AC) demonstrate the simultaneous impact of various parameters on surface quality.

From the ANOVA analysis:

- **Laser Power (A)** This is contrary to expectations and shows that kerf width, taper and surface roughness

have the most significant correlation across all the responses.

- The **cutting speed (B)** significantly influences kerf width and surface roughness, albeit in an escalated manner.
- **Gas Pressure (C)** It is also ascribed a minor influence, mostly in reducing the range of kerf taper and increasing surface roughness.
- The **Quadratic Effects** (A^2, B^2) to further prove the reductionist nature of the medium and further show how the process parameters are not directly proportional to the responses.

Consequently, it becomes paramount to select the laser power and cutting velocity sensitively and apply the appropriate pressure of the gas to minimize the kerf width and taper, as well as surface roughness of AISI 304 stainless-steel.

5.0 Conclusion

The goal of this study was to examine the effect of different laser cutting process parameters, like laser power, cutting speed, gas pressure, and focal location, on the quality of cuts for AISI 304 stainless steel in terms of kerf width, kerf taper, and surface roughness. Based on the results of the ANOVA analysis, the following conclusions can be drawn:

5.1 Optimal Process Parameters

- Laser power significantly impacts surface characteristics like kerf width, taper, and roughness. The outcome of the study also converges to the setting of laser power to around 3000W, which results in the smallest kerf width and improved surface roughness.
- The optimal cutting speed that allowed for a balance between accuracy and surface finish was determined to be 4500 mm/min, especially for the thinner grades of AISI 304 steel (1.5mm to 2mm).
- Gas pressure of 0.8MPa is ideal for cutting with low kerf taper and surface roughness, as it effectively ejects molten material.
- It is identified that holding the focal position to -1.5 mm ensures that the laser is accurately focused onto the material, which reduces the kerf width and taper and improves surface finish.

5.2 Kerf Width and Taper

- Laser power and cutting speed are found to be relevant parameters in determining kerf width and taper. The bottom kerf width was typically less than the top kerf width, hence Kerf taper was positive.
- The expression of Laser power is quadratic in nature, reveals that greater power produces wider kerfs and greater kerf taper. It propounds that high-power yields undesirable tapering of the cuts.
- Comparing curved profiles and laser power or cutting speed, a low value of kerf taper (0.8455°) is obtained for curved cuts with 2mm thick sheets. It indicates that the curved cuts have fewer taper deformations because of uniform ablation.

5.3 Surface Roughness

- Surface roughness on cut edges is determined by laser power and cutting speed. An increase in laser power escalates surface roughness due to melting and uneven solidification.
- For 1.5mm thick straight profile cuts, a maximum surface roughness of 1.621µm is achieved with cutting parameters of 3000W power, 4500 mm/min cutting speed, and 0.8 MPa gas pressure.
- Curved profiles exhibit improved surface quality over straight profiles, with smoother edges due to continuous laser cutting lines.

5.4 Final Recommendations

To achieve the best cutting results for AISI 304 stainless steel:

- Optimal parameters recorded to minimise kerf breadth, taper, and surface roughness (for material thicknesses between 1.5 mm and 2 mm) are a laser power of 3000W, a cutting speed of 4500 mm/min, a gas pressure of 0.8 MPa, and a focal location -1.5mm.
- The curved profiles exhibit superior kerf width, taper, and surface quality, rendering them suitable for applications with sharp edges.
- Thick materials necessitate optimal process parameters, especially laser power, owing to the augmentation of kerf width, taper, and surface roughness.
- This study envisages the feasibility of achieving optimal laser cutting conditions for producing thin

cuts in AISI 304 stainless steel across varied material thicknesses and profiles.

6.0 References

1. Ahmed N, Rehman AU, Ishfaq K, Naveed R, Moiduddin K, Umer U, Ragab AE, Zabidi A. Achieving the minimum roughness of laser milled micro-impressions on Ti 6Al 4V, Inconel 718, and Duralumin. Materials. 2020; 13(20):4523. https://doi.org/10.3390/ma13204523 PMid:33053899 PMCid:PMC7601468.
2. Brecher C, Emonts M, Eckert M, Weinbach M. Double-sided irradiation for laser- assisted shearing of ultra-high-strength steels with process-integrated hardening. Procedia CIRP. 2014; 56:1427-1435. https://doi.org/10.1016/j.phpro.2014.08.074
3. Genna S, Menna E, Rubino G, Tagliaferri V. Experimental investigation of industrial laser cutting: The effect of the material selection and the process parameters on the kerf quality. Appl Sci. 2020; 10(14):4956. https://doi.org/10.3390/app10144956
4. Giorgi C, Furlan V, Demir AG, Tallarita E, Candiani G, Previtali B. Laser micropolishing of AISI 304 stainless steel surfaces for cleanability and bacteria removal capability. Appl Surf Sci. 2017; 406:199-211. https://doi.org/10.1016/j.apsusc.2017.02.083
5. Jadhav A, Kumar S. Laser cutting of AISI 304 material: An experimental investigation on surface roughness. Mater Res Lett. 2019; 5(3):429-437. https://doi.org/10.1080/2374068X.2019.1622297
6. Kumar M, Aravindan K, Vinoth J, Kumar TS. Effect of post-fabrication treatments on surface residual stresses of additive manufactured stainless steel 316L. FME Transactions. 2021; 49(1):87-94. https://doi.org/10.5937/fme2101087B
7. M'Saoubi R, Outeiro J, Changeux B, Lebrun JL, Dias AM. Residual stress analysis in orthogonal machining of standard and resulfurized AISI 316L steels. J Mater Process Technol. 1999; 96(1-3):225-233. https://doi.org/10.1016/S0924-0136(99)00359-3
8. Mahrle A, Borkmann M, Pfohl P. Factorial analysis of fibre laser fusion cutting of AISI 304 stainless steel: Evaluation of effects on process performance, kerf geometry, and cut edge roughness. Materials. 2021; 14(10):2669. https://doi.org/10.3390/ma14102669 PMid:34069714 PMCid:PMC8161254.
9. Manohar M. CO_2 laser beam cutting of steels: Material issues. Journal of Laser Applications. 2006; 18(2):101-112. https://doi.org/10.2351/1.2193173
10. Maurotto A, Scenini F, Kraemer BF. Laser irradiation effects in simulated laser- assisted machining of type 316L SS. J Manuf Mater Process. 2018; 2(3):45. https://doi.org/10.3390/jmmp2030045
11. Mousavi SAAAA, Gharedaghi A, Mastoori M. Metallurgical investigations of laser welding of AISI 304 stainless steel. Materials Science Forum. 2008; 580-582:41-44. https://doi.org/10.4028/www.scientific.net/MSF.580-582.41
12. Outeiro J, Dias AMPG, Lebrun JL, Astakhov VP. Machining residual stresses in AISI 316L steel and their correlation with the cutting parameters. Mater Sci Technol. 2002; 6(2):251-270. https://doi.org/10.1081/MST-120005959
13. Pessoa D, Herwig P, Wetzig A, Zimmermann M. Influence of surface condition due to laser beam cutting on the fatigue behaviour of metastable austenitic stainless steel AISI 304. Eng Fract Mech. 2017; 185:227-240. https://doi.org/10.1016/j.engfracmech.2017.05.040
14. Pramanik D, Kuar AS, Sarkar S, Mitra S. Optimisation of edge quality on stainless steel 316L using low-power fibre laser beam machining. Mater Res Lett. 2020; 7(1):42-53. https://doi.org/10.1080/2374068X.2020.1745734
15. Tsai M, Wu L. Multi-objective optimisation of Nd: YAG laser drilling of optical-grade acrylic plate using Taguchi-based grey relational analysis. Mater. 2022; 15(24):8998. https://doi.org/10.3390/ma15248998 PMid:36556804 PMCid: PMC9785554.
16. Maniyar KG, Ingole DS. Multi-response optimisation of EDM process parameters for aluminium hybrid composites by GRA. Mater Today Proc. 2018; 5:1983643. https://doi.org/10.1016/j.matpr.2018.06.347
17. Maniyar KG, Ingole DS. Investigation of EDM process parameters for hybrid metal matrix composites. IOP Conf Ser Mater Sci Eng. 2018; 377:012204. https://doi.org/10.1088/1757-899X/377/1/012204
18. Maniyar KG, Ingole DS. Mathematical modelling and optimisation of EDM process parameters for aluminium hybrid composites. Mater Today Proc. 2018; 5:27700-277009. https://doi.org/10.1016/j.matpr.2018.10.004
19. Maniyar KG, Ingole DS. Influence of EDM control factors for aluminium hybrid Composites. Lect Notes Multidiscipl Indust Eng. 2018; 275-284. https://doi.org/10.1007/978-3-319-76276-0_27
20. Maniyar KG. An experimental analysis of aluminium hybrid metal matrix composites, Mater Today Proc. 2024. https://doi.org/10.1016/j.matpr.2024.01.021
21. Maniyar KG, Marode RV, Chikalthankar SB. Optimisation of EDM process parameters on MRR and

TWR of Tungsten Carbide by Taguchi method. Int J Eng Adv Technol. 2016; 5:112-116. https://doi.org/10.1016/j.matpr.2024.01.021
22. Maniyar KG. Analysis of EDM process parameters on material removal rate of WC. 2nd Nat Conf Recent Inno Sci Eng. 2017; 5(9):37-39.
23. Maniyar KG, Agrawal SK, Ingole DS. Optimisation of multiple performance characteristics in EDM: A critical literature review. Int J Innov Technol Explor Eng. 2016; 5(10):27-33.
24. Maniyar KG, Deore HV. Design and testing of carbon fibre composite material with comparative analysis. Int Res J Eng Tech. 2020; 7(8):1120-1122.
25. Maniyar KG, Ingole DS. Current research development in machining of hybrid metal matrix composites: A review. Int J Recent Innov Trends Comput Commun. 2016; 4(7):150-154.
26. Jadhav PA, Maniyar KK, Evaluation and characterisation of aluminium silicon carbide Metal Matrix Composites. AIP Conf Proc. 2024. https://doi.org/10.1063/5.0227945
27. Maniyar K, Jadhav P, Biradar R, Gawande J. An experimental study of process parameters for nano composites. NanoWorld J. 2024; 10(S1):S209-211.
28. Maniyar K, Jadhav P, Biradar R, Gawande J. Effect of nano-lubricants on journal bearing for performance enhancement. NanoWorld J. 2024; 10(S1):S206-208.
29. Maniyar K, Suhane S. Parametric analysis of electric discharge machining for nano composites. NanoWorld J. 2024; 10(S1):S63-65.
30. Maniyar K, Puri A, Pawar P, Patil V, Jadhav P, Patil G, *et al*. The comprehensive study for the machining of metal matrix composites. AIP Conf Proc. 2024; 3196:040005. https://doi.org/10.1063/5.0227955
31. Maniyar K, Warke P, Jadhav P, Waware S, Harsur S, Biradar R. An extensive study of mechanical properties and tribological characteristics for hybrid composites. AIP Conf Proc. 2024; 3203:030038-8. https://doi.org/10.1063/5.0224994
32. Maniyar K, Pawar P, Kolhe P, Ingale M, Patil P, Sarode G. The comprehensive study of synthesis and characterisation of hybrid nano fluids. AIP Conf Proc. 2024; 3149: 030048. https://doi.org/10.1063/5.0224988
33. Ghutepatil PR, Khapare S, Barve Joshi R, Maniyar KG. A critical review of nanotechnology in various fields of engineering. AIP Conf Proc. 2024; 3149:030002. https://doi.org/10.1063/5.0224984
34. Thamke V, Saravade N, Banarase S, Maniyar K. Seismic performance and cost analysis of AAC blocks vs. fly ash bricks: A comparative study utilising STAAD pro. AIP Conf Proc. 2024; 3196:060006. https://doi.org/10.1063/5.0227895
35. Banarase S, Banarase M, Saravade N, Thamke V, Maniyar K. Evaluation of concrete building strengthening through non-destructive testing methods - A case study. AIP Conf Proc. 2024; 3196:040001. https://doi.org/10.1063/5.0227927
36. Maniyar K, Harsur SK, Shinde SN, Shaaikh JA, Chandan MN, Rupanar S. An experimental investigation of machining parameters on aluminium composites. J Polym Compos. 2024; 12(06):8-13.
37. Maniyar K, Harsur SK. Experimental findings of the EDM process parameters for metal matrix composites. J Polym Compos. 2024; 12(06):14-18.
38. Saravade N, Sedani C, Maniyar K, Nandkishore D, Deshmukh S, Rupanar S, Gidhad B, Surase S. Study on heavy machinery utilising the most recent technologies for excavation of road construction and mining. J Mines Met Fuels. 2024; 72(7):667-673. https://doi.org/10.18311/jmmf/2024/45327
39. Patil GH, Mishra E, Maniyar K, Rawoot M, Satarkar MFAR. Study on prediction of lightning impulses on transmission line tower due to harsh field and variable working condition, environmental condition and tower footing resistances. J Mines Met Fuels. 2024; 72(7):763-769. https://doi.org/10.18311/jmmf/2024/45322
40. Jathar A, Maniyar K, Nawghare B, Ansari S, Patil PG, Mali C, Biradar R, Deshmukh S, Surase S, Gaikar S. An extensive study of nanomaterials and nanotechnology in the various fields of engineering. J Mines Met Fuels. 2024; 72(10):1067-1074. https://doi.org/10.18311/jmmf/2024/45658
41. Nawghare B, Maniyar K, Jathar A, Mali C, Pawar D, Jadhav SP, Deshmukh S, Rupanar S, Biradar R, Gawande J, Warghat S. An extensive study of nano fluids and their applications in real life. J Mines Met Fuels, 2024; 72(10):1119-1124. https://doi.org/10.18311/jmmf/2024/45407
42. Raut P, Maniyar K, Kakade S, Rupanar S, Bhalake S, Mali C, Deshmukh S, Biradar R. A comprehensive analysis of the synthesis, properties and uses of nanofluid. J Mines Met Fuels. 2024; 72(9):965-971. https://doi.org/10.18311/jmmf/2024/45524 https://doi.org/10.18311/jmmf/2024/45524
43. Warghat S, Sedani C, Rasane A, Maniyar K, Dhanwate V, Jadhav SP, Deshmukh S, Gawande J, Biradar R. An extensive study of metal matrix composites and their various properties for different uses. J Mines Met Fuels. 2024; 72(9):949-955. https://doi.org/10.18311/jmmf/2024/45554

44. Mali C, Maniyar K, Rupanar S, Jathar A, Nawghare B, Kakade N, Modak G, Bhambere V, Deshmukh S, Gawande J, Biradar R. An analysis of nanoparticles in composite materials. J Mines Met Fuels. 2024; 72(11):1215-1223. https://doi.org/10.18311/jmmf/2024/45579
45. Patil G, Mishra E, Maniyar K, Warke P. Four-quadrant operation of induction motor using h-bridge in harsh and noxious environment field with dust, voltage fluctuation and major load variations. J Mines Met Fuels. 2024; 72(11):1225-1231. https://doi.org/10.18311/jmmf/2024/45557
46. Mhaske M, Gidhad B, Maniyar K, Ghuge G. The role of linear algebra in developing machine learning solutions. 2024 3rd International Conference for Advancement in Technology (ICONAT), GOA, India; 2024. p. 1-5. https://doi.org/10.1109/ICONAT61936.2024.10775140 PMid:38258445
47. Ansari S, Vaidya K, Kadu A, Rokade A, Maniyar K. (2025). A comprehensive study on modern electronic technologies in the field-based engineering industry. J Mines Met Fuels. 2025; 73(2):455-465. https://doi.org/10.18311/jmmf/2025/47122
48. Ghodke BS, Maniyar K. Using GeoGebra and SageMath to assist engineering students in tracing different curves and solving numerical methods, communications on applied nonlinear analysis. 2025; 32(6). https://doi.org/10.52783/cana.v32.3310
49. Kakade N, Gaikwad D, Sayyad S, Sedani C, Sayyad F, Rupanar S, Bangar N, Maniyar K, Thermal analytical characterization of *Gymnema sylvestre* using TGA-DTA technique, communications on applied nonlinear analysis. 2025; 32(6-7). https://doi.org/10.52783/cana.v32.3492
50. Maniyar K, Rupanar S, Sayyad F, Sedani C, Gawande J, Pawar P. An analysis of machining parameters for metal matrix composite. J Polym Compos. 2025; 13(02):76-85.
51. Mishra E, Jog P, Bugade VS, Patil GH, Jarad RS, Kulkarni B, Maniyar K, Case study on role of solar energy in greenhouse gas emissions reduction in India, J Inf Syst Eng Manag. 2025; 10(19):462-471. https://doi.org/10.52783/jisem.v10i19s.3058
52. Patil S, Kute U, Jakhete M, Ansari S, Maniyar K, Chimkode S, Modak G, Bhambere V, Kolte R, Warghat S, Desai S, Mathur J, Warke P, Patil G, Mishra E. The role of internet of things, cloud computing, artificial intelligence and robotics in the fourth industrial revolution. J Mines Met Fuels. 2025. https://doi.org/10.18311/jmmf/2025/47334
53. Kakade N, Dashrath A, Kharche Y, Choudhari R, Sedani C, Rupanar S, Gaikwad D, Mane J, Biradar R, Jakhete M, Ghodke P, Yadav M, Maniyar K, Patil G. Examining experimentally the impact of spot-welding process variables on metal matrix composites. J Polym Compos. 2025; 13(05).
54. Mishra E, Patil GH, Chavan SD, Jarad RS, Satarkar M, Thakare M, Maniyar K. Analysis of the Impact of STATCOM on distance relay using MATLAB. Jo Mines Met Fuels. 2025; 73(3):743-750. https://doi.org/10.18311/jmmf/2025/48052
55. Choudhari RM, Chopde PV, Kharche NA, Shekokar SR, Kharche YA, Warke P, Maniyar K, Patil G. Determinant factors for the development of rural entrepreneurship. J Inform Systems Eng. 2025; 10(25):111-118. https://doi.org/10.52783/jisem.v10i25s.3951
56. Patil G, Upasani S, Vaidya H, Desai K, Satarkar MFAR, Mishra E, Maniyar, K DTMF Phone call control home appliance using Arduino and GSM module and home automation. J Inform Systems Eng. 2025; 10(25):249-257. https://doi.org/10.52783/jisem.v10i25s.3976
57. Kadam J, Phadtare G, Pawar A, Maniyar K Offline signature verification using Siamese neural network. J Inform Systems Eng. 2025; 10(26):431-439. https://doi.org/10.52783/jisem.v10i26s.4245
58. Garad RN, Hudgikar SRK, Maniyar K. An extensive study on the optimized piston bowl with spiral grooves for the CI engine. J Mines Met Fuels. 2025; 73(5):1389–1394. https://doi.org/10.18311/jmmf/2025/48016
59. Choudhari RM, Adhaye AM, Sulakhe VN, Warke PS, Maniyar KG. An Analysis of tensile strength and performance of resistance spot welding parameters for HSLA 355 stainless steel. J Mines Met Fuels. 2025; 73(5):1409–1418. https://doi.org/10.18311/jmmf/2025/48684
60. Warke PS, Chaudhari DM, Naik VS, Patil DD, Dhokale SS, Maniyar KG, Patil GH. Wet scrubber system for exhaust gas emission reduction. J Mines Met Fuels. 2025; 73(5):1331–1341. https://doi.org/10.18311/jmmf/2025/48623,
61. Maniyar K, Puri A, Suhane S, Deshmukh S, Modak G, Biradar R. An Experimental Performance of EDM Process Parameters for Aluminum Composites. In: Joseph DPVJ, Thangaraju K. editors. Proceedings of the International Conference on Emerging Multifunctional Materials and Devices for Sustainable Technologies. IEMDST. Springer, Singapore; 2024. https://doi.org/10.1007/978-981-96-5863-3_44
62. Maniyar K, Saravade N, Suhane S, Deshmukh S, Modak G, Biradar R. Investing Experimental Effect of Welding Parameters in Friction Stir Welding on Aluminium Alloy. In: Joseph DPVJ, Thangaraju K. editors. Proceedings of the International Conference on Emerging Multifunctional Materials and Devices for Sustainable Technologies. IEMDST. Springer, Singapore; 2024. https://doi.org/10.1007/978-981-96-5863-3_45
63. Kulkarni H, Patel P, Jape V, Soman A, Mishra E, Maniyar K, Patil G. The hybrid PSO-ANN methodology for

enhancing net load prediction in modern power systems. J Mines Met Fuels. 2025; 73(6):1833–1838. https://doi.org/10.18311/jmmf/2025/49104

64. Kulkarni H, Jape V, Shiralkar A, Soman A, Lokhande N, Bhandare D, Maniyar K, Patil G. Design of an intelligent PLC-based protection for power transformers with auto-re-closer. J Mines Met Fuels. 2025; 73(7):1915–1923. https://doi.org/10.18311/jmmf/2025/49137
65. Kulkarni H, Jape V, Shiralkar A, Soman A, Bugde V, Bhandare D, Maniyar, K, Patil G. The role of electric vehicles in a sustainable future and environment. J Mines Met Fuels. 2025; 73(7):1925–1933. https://doi.org/10.18311/jmmf/2025/49119
66. Patil G, Dabhade A, Jog P, Bugade V, Patil M, Gurav J, Desai K, Maniyar K, Mishra E, Kulkarni H, Patel P, Jakhete M, Ghodke P, Yadav M. Comprehensive analysis of solar photovoltaic system power inverter topologies. J Mines Met Fuels. 2025; 73(7):1935–1943. https://doi.org/10.18311/jmmf/2025/49149
67. Mukadam S, Sulakhe V, Kaware K, Maniyar K. A comprehensive study on challenges in gear manufacturing using fused deposition modeling. J Mines Met Fuels. 2025; 73(7):1973–1985. https://doi.org/10.18311/jmmf/2025/49194
68. Chimkode S, Mane J, Jakhete M, Moharil U, Sedani C, Rao N, Garad R, Rupanar S, Kakade N, Choudhari R, Bhambere V, Modak G, Paliwal R, Desai S, Maniyar K, Patil G, Mishra E, Ghodke P, Dixit S, Yadav M. Recent advancements in the field of nanotechnology using artificial intelligence, data science and machine learning. J Mines Met Fuels. 2025; 73(7):1987–1994. https://doi.org/10.18311/jmmf/2025/49272
69. Pawar NR, Hudgikar SRK, Sarnobat SS, Channapattana SV, Maniyar KG. Optimization of multi-cylinder four-stroke SI engine performance under magnetic field interference using CNG fuel. J Mines Met Fuels. 2025; 73(7):2009–2013. https://doi.org/10.18311/jmmf/2025/49144
70. Mahamulkar V, Jadhav S, Pawar A, Wagh D, Bhaware A, Jadhav S, Patil G, Maniyar K, Ghodke P, Mishra E. Dynamic wireless power transmission system for EV. J Mines Met Fuels. 2025; 73(7):2155–2161. https://doi.org/10.18311/jmmf/2025/49252
71. Lodha K, Mohod S, Yadav S, Tomar P, Thawali B, Jahagirdar A, Burande P, Patil G, Maniyar K. Innovative algorithms for state-of-charge estimation in electric vehicle batteries. J Mines Met Fuels. 2025; 73(7):2207–2220. https://doi.org/10.18311/jmmf/2025/49439
72. Warbhe R, Jadhav P, Kamble P, Londhe N, Rajguru P, Patil G, Maniyar K, Ghodke P. The role of Radio Frequency Identification (RFID) technology in mining industries and other fields. J Mines Met Fuels. 2025; 73(7):2233–2240. https://doi.org/10.18311/jmmf/2025/49174
73. Banarase S, Mane J, Kharche Y, Choudhari R, Sedani C, Rupanar S, Kakade N, Jakhete M, Ghodke P, Yadav M, Bhambere V, Modak G, Maniyar K, Patil G. An experimental investigation of process parameters for aluminum alloy composites. J Polym Compos. 2025; 13(04).